Probing the Spatial Proximities among Acid Sites in Dealuminated H-Y Zeolite by Solid-State NMR Spectroscopy

Shenhui Li,[†] Shing-Jong Huang,[‡,§] Wanling Shen,[†] Hailu Zhang,[†] Hanjun Fang,[†] Anmin Zheng,[†] Shang-Bin Liu,*[,‡] and Feng Deng*[,†]

State Key Laboratory of Magnetic Resonance and Atomic and Molecular Physics, Wuhan Center for Magnetic Resonance, Wuhan Institute of Physics and Mathematics, Chinese Academy of Sciences, Wuhan 430071, China, and Institute of Atomic and Molecular Sciences, Academia Sinica, P.O. Box 23-166, Taipei 10617, Taiwan

Received: April 22, 2008; Revised Manuscript Received: June 26, 2008

A comprehensive study has been made to probe the spatial proximities among different acid sites in dealuminated H-Y zeolites modified with various degrees of calcination, steam, and acid treatments by using a variety of different solid-state NMR techniques, including multinuclear MAS NMR and two-dimensional ^{1}H double-quantum (DQ) MAS NMR spectroscopy. The effects of dealumination treatments on the nature, concentration, and location of extraframework Al species in H-Y zeolites were followed by ^{1}H DQ MAS NMR of hydroxyl protons in conjunction with ^{1}H, ^{27}Al, and ^{29}Si MAS NMR results. It was found that the extraframework AlOH species (Lewis acid sites) are always in close proximity to the bridging AlOHSi hydroxyls (Brønsted acid sites) on the framework of dealuminated H-Y zeolites prepared by thermal and hydrothermal treatments, indicating the presence of a Brønsted/Lewis acid synergy effect. However, such an effect is absent in acid-treated H-Y zeolites, as also confirmed by ^{13}C CP/MAS NMR of adsorbed 2-^{13}C-acetone.

1. Introduction

The catalytic performances (i.e., activity and selectivity) of solid acid catalysts, such as zeolites, are mainly dictated by their acid properties,[1−5] namely, the type (Brønsted vs Lewis), concentration, strength, and location (intra- vs extracrystalline) of acid sites.[6] As such, preparation of an active and stable catalyst normally invokes postsynthesis modification and/or treatment of the as-synthesized material.[1−5,7] Among them, dealumination treatments,[2,8] which allow for adjustment of the framework Si/Al ratio of acid catalysts by thermal/hydrothermal treatment,[9] acid leaching,[10] or chemical treatments with silicon tetrachloride[11,12] or ammonium hexafluorosilicate (AHFS),[12−14] are the most common practice. In general, the dealumination process is normally accompanied by hydrolysis of the framework Si−O−Al linkages, eventually resulting in the release of aluminum atoms from the framework and hence leading to the formation of extraframework Al (EFAL) species. Oxoaluminum cations such as AlO^{+}, $Al(OH)_2^{+}$, and $AlOH^{2+}$ and neutral polymeric species such as AlOOH, $Al(OH)_3$, and Al_2O_3 have been proposed as the possible forms of EFAL species.[15]

In general, the catalytic activity observed for dealuminated zeolites is normally higher than that of their respective parent samples.[16−25] For example, Mota and co-workers[20] found that the H/D exchange rate of 3-methylpentane increased by about 20-fold at 100 °C, when EFAL species were present in USY zeolite. Biaglow et al.[21] also observed a 10-fold increase in catalytic activity during *n*-hexane cracking over dealuminated faujasite (FAU) zeolites. Although the nature and detailed structures of EFAL remain unclear and debatable issues mainly due to lack of direct experimental evidence, some reports have attributed such activity enhancement observed in dealuminated zeolites to the synergic effect between Brønsted and Lewis acid sites.[22−25]

As the EFAL species (Lewis centers) interact with the electron pairs of the framework oxygen atoms, they tend to delocalize the electron density near the Brønsted acid site, thus resulting in an increase in acidity. Such a synergic effect between Brønsted and Lewis acid sites has been reported in various dealuminated zeolites, such as H-Y, H-MOR, H-ZSM-5, H-ZSM-11, and SAPO-5.[26−29] For example, Mirodatos et al.[29] suggested that the superacid sites in dealuminated mordenite zeolite mainly arise from the interactions between protonic sites and polymeric oxoaluminum species located in the zeolite channels, invoking a partial electron transfer from the Brønsted proton (bridging hydroxyls) to the oxoaluminum species (such as AlO^{+} and AlOOH). As a result, the increase in the acid strength of the acid site is directly reflected by the increase in the O−H bond length of the bridging hydroxyl groups, much similar to that in superacid systems, such as $AlCl_3$−HCl and SbF_5−HF.[30]

While solid-state ^{29}Si and ^{27}Al MAS NMR have been widely used for structural characterization of zeolites and molecular sieve materials,[31] acidity characterization normally invokes detection of the bridging hydroxyl OH groups either directly by ^{1}H MAS NMR[32] or through ^{13}C,[33−35] ^{15}N,[36] and/or ^{31}P[6,7,37−43] MAS NMR of adsorbed base molecules as probes. Presumably, the presence of EFAL should lead to a downfield shift in the ^{1}H chemical shift of bridging hydroxyls; however, this phenomenon was not readily observed in earlier ^{1}H MAS NMR studies.[32] As such, more sophisticated multinuclear double- and triple-resonance NMR methods, such as REDOR (rotational echo double resonance),[44] HETCOR (heteronuclear correlation),[45] TRAPDOR (transfer of populations in double reso-

* To whom correspondence should be addressed. (F.D.) E-mail: dengf@wipm.ac.cn. Fax: +86-27-87199291. (S.-B.L.) E-mail: sbliu@sinica.edu.tw. Fax: +886-2-23620200.

† Chinese Academy of Sciences.

‡ Academia Sinica.

§ Present address: Department of Chemistry, National Taiwan University, Taipei 10617, Taiwan.

10.1021/jp803494n CCC: $40.75
Published on Web 08/20/2008

nance),[46] and MQMAS (multiple-quantum magic-angle-spinning)[47] techniques, have been used to characterize the local Al environments of dealuminated aluminosilicate catalysts[39,40,42] and to identify the EFAL species.[14] For example, ^{1}H, ^{27}Al, and ^{31}P MAS NMR, ^{31}P → ^{1}H CP, and ^{1}H{^{27}Al}, ^{31}P{^{27}Al} TRAPDOR, and ^{1}H/^{31}P/^{27}Al CP-TRAPDOR NMR have been used to identify acid sites in various solid acid catalysts, such as H-Y, H-ZSM-5, Al-MCM-41, using TMP and/or trimethylphosphine oxide (TMPO) as probes.[6,37−42] By using ^{1}H, ^{19}F, and ^{27}Al MAS, two-dimensional (2D) ^{19}F{^{27}Al} and ^{27}Al{^{19}F} HETCOR, ^{19}F{^{27}Al} TRAPDOR, and ^{27}Al{^{19}F} REDOR NMR, Kao and co-workers[14] have demonstrated that the detailed reaction pathways and the nature of EFAL species formed during AHFS dealumination in zeolites (such as H-Y, H-MOR, and H-Beta) may be determined. In addition, the spatial connectivity among various acid sites in zeolites can be directly observed by using solid-state ^{1}H double-quantum (DQ) MAS NMR.[48] On the basis of ^{1}H DQ MAS NMR and ^{13}C MAS NMR of adsorbed 2-^{13}C-acetone, we have demonstrated[49] that detailed spatial proximities between Brønsted and Lewis acid sites in dealuminated H-Y zeolites can be obtained and that the synergic effect between the two adjacent Brønsted and Lewis acid sites normally results in a notable increase in the acid strength of the zeolitic catalyst. Furthermore, by combining these results with results obtained from density functional theory (DFT) calculations, detailed structures of the EFAL species as well as the Brønsted/Lewis acid synergy were also revealed for the first time. It was concluded that extraframework $Al(OH)_3$ and $AlOH^{2+}$ species located in the supercages and $AlOH^{2+}$ species present in the sodalite cages are the preferred Lewis acid sites in dealuminated H-Y zeolite. Moreover, it is the coordination of the EFAL species to the oxygen atoms nearest to the framework Al, rather than direct interactions between EFAL species and Brønsted acid sites, that is responsible for acidity enhancement.

In this work, we aim to explore the spatial proximities among Brønsted and Lewis acid sites in H-Y zeolite treated with various dealumination methods and at different levels of dealumination by means of ^{1}H, ^{27}Al, and ^{29}Si MAS NMR in conjunction with ^{1}H DQ MAS NMR techniques. The Brønsted/Lewis acid synergy effect on the acid strength of the dealuminated H-Y zeolites treated under various conditions is also confirmed by ^{13}C MAS NMR of adsorbed 2-^{13}C-acetone.

2. Experimental Section

2.1. Preparation of NH_4-Y and H-Y Zeolites. Powdered, binderless Na-Y zeolite (Si/Al = 2.8; Strem Chemical Inc.) was exchanged in a 1.0 mol/L aqueous solution of NH_4Cl at 353 K for 4 h and then washed with distilled water. This process was repeated several times till the absence of chloride ion in the sample. Subsequently, the resultant NH_4-Y zeolite was first dried in air at 353 K overnight and then subjected to dehydration treatment under a vacuum ($<10^{-5}$ Torr; 1 Torr = 133.32 Pa). To avoid dealumination of the zeolite during dehydration, the temperature was first ramped from room temperature (rt = 298 K) to 373 K at a rate of 1 K/min and then from 373 to 673 K at a rate of 1.6 K/min and eventually kept at the elevated temperature for ca. 8 h. Finally, the H-Y zeolite was obtained. Additional experiments by ^{27}Al MAS NMR revealed (see the Supporting Information, Figure S1) the absence of extraframework Al in both Na-Y and H-Y zeolites and that the two parent samples have nearly the same Si/Al ratio, as determined by ^{29}Si MAS NMR (see the Supporting Information, Figure S2), of 2.8.

2.2. Dealumination Treatments. To explore the spatial proximities among acid sites in H-Y zeolite, samples subjected to three different dealumination methods, viz., calcination, steaming, and acid-leaching treatments, under various treatment conditions were prepared and examined.

2.2.1. Calcined H-Y Zeolites. Calcined H-Y samples were prepared by packing the NH_4-Y zeolite in a shallow bed configuration on a quartz crucible and then subjecting it to calcination treatment in dry air at specified conditions in a tube furnace. Typically, the heating temperature was raised from rt to a target temperature (400, 500, 600, and 700 °C) at a rate of 2.5 °C/min and then kept at the same temperature for 4 h. The calcined samples so prepared are denoted hereafter as CAL-*X*, where *X* (400, 500, 600, and 700 °C) represents the final calcination temperature (°C).

2.2.2. Steamed H-Y Zeolites. A ca. 1 g sample of the H-Y zeolite was placed in a tubular quartz reactor (i.d. 1 in.) such that the sample bed had a typical height of ca. 6 mm. Subsequently, each sample was exposed to a flow of 100% steam while the temperature was ramped from rt to a target temperature (350, 450, and 550 °C) at a rate of 3 °C/min and then maintained at the final temperature for 2 h. The steamed H-Y samples so prepared are denoted hereafter as STY-*X*, where *X* (350, 450, and 550 °C) represents the final hydrothermal treatment temperature (°C).

2.2.3. Acid-Treated H-Y Zeolites. Dealuminated H-Y zeolites prepared by acid-leaching were obtained by refluxing the H-Y zeolite with different oxalic acid concentrations (*Y*) under stirring conditions at a temperature of 333 K for 3 h. Subsequently, each dealuminated sample was washed thoroughly with deionized water and then dried overnight at 383 K. The acid-treated H-Y samples so prepared are denoted hereafter as OXA-*Y*, where *Y* (0.2, 0.8, and 1.4 mol/L) represents the concentration of the oxalic acid solution (mol/L).

2.3. Solid-State NMR Experiments. All NMR experiments were carried out on a Varian InfinityPlus-400 spectrometer, corresponding to the Larmor frequencies of 400.1, 104.3, 79.5, and 100.5 MHz for ^{1}H, ^{27}Al, ^{29}Si, and ^{13}C nuclei, respectively. Prior to each ^{1}H MAS NMR experiment, ca. 0.2 g of the sample was packed into a glass tube, which was later connected to a vacuum line. Subsequently, dehydration of the sample was carried out by raising the temperature of the furnace beneath from rt to 673 K at a rate of 1 K/min under a vacuum ($<10^{-5}$ Torr) for at least 8 h. The sealed sample tube was opened under a N_2 environment in a glovebox, and the sample was transferred into a 5 mm ZrO_2 MAS rotor and then sealed with a gastight Kel-F cap. A $\pi/2$ pulse length of 3.57 μs, a recycle delay of 5 s, and a sample spinning rate of 10 kHz were used for ^{1}H MAS NMR experiments. ^{13}C CP/MAS NMR of adsorbed acetone was used to characterize the acid strength of various dealuminated H-Y zeolites. Prior to the ^{13}C CP/MAS NMR experiment, ca. 0.2 mmol/g ^{13}C isotope-enriched 2-^{13}C-acetone was introduced and frozen onto the dehydrated catalyst with liquid N_2. Finally, the sample was transferred into the NMR rotor under a dry N_2 atmosphere in a glovebox. Typically, the ^{1}H → ^{13}C CP/MAS NMR measurements were performed with a contact time of 2 ms, a recycle delay of 4 s, and a sample spinning rate of 7 kHz, ^{29}Si MAS NMR spectra with high-power proton decoupling were recorded using a $\pi/4$ pulse length of 2 μs, a recycle delay of 80 s, and a spinning rate of 5 kHz, and ^{27}Al MAS NMR spectra were recorded with a pulse length of 0.5 μs ($<\pi/12$), a recycle delay of 1 s, and a spinning rate of 6 kHz. Unlike the ^{1}H and ^{13}C NMR spectra, which were obtained from dehydrated samples, fully hydrated samples were used during the ^{27}Al and ^{29}Si MAS NMR measurements. The

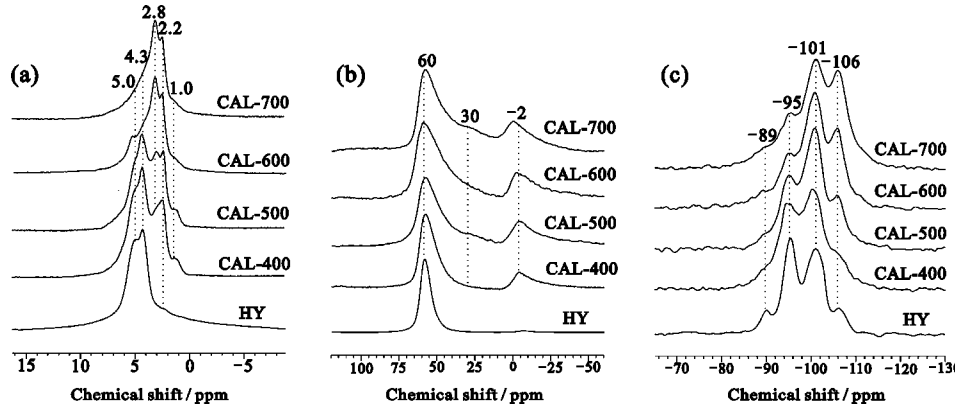

Figure 1. (a) ^{1}H, (b) ^{27}Al, and (c) ^{29}Si MAS NMR spectra of parent H-Y and various dealuminated H-Y zeolites prepared with different calcination temperatures (400−700 °C).

TABLE 1: List of Si/Al and Al_F/Al_{total} Ratios and Spectral Assignments for the Parent and Various Dealuminated H-Y Zeolites

			relative peak area (%)[c]				
sample	Si/Al[a]	Al_F/Al_{total}[b] (%)	AlOHSi (5.0 ppm)	AlOHSi (4.3 ppm)	AlOH (2.8 ppm)	SiOH (2.2 ppm)	AlOH (1.0 ppm)
H-Y	2.8	100	47.3	49.6		3.1	
CAL-400	3.0	80.2	20.6	40.3	22.1	13.7	2.3
CAL-500	3.5	79.2	18.8	39.3	21.3	17.9	2.7
CAL-600	4.6	58.6	13.8	25.7	37.1	20.8	2.6
CAL-700	5.3	32.1	8.1	21.8	41.3	26.4	2.4
STY-350	3.8	80.3	17.5	41.7	24.7	14.0	2.1
STY-450	4.3	60.1	14.6	30.2	36.4	16.1	2.7
STY-550	5.2	36.2	8.1	24.8	48.1	15.8	3.2
OXA−0.2	2.8	95.6	45.3	44.6	1.4	8.8	
OXA−0.8	3.6	69.9	29.7	42.7	6.0	21.6	
OXA−1.4	6.1	46.7	15.9	35.2	22.0	26.9	

[a] Si/Al ratios (±3%), as determined by ^{29}Si MAS NMR. [b] Atomic ratios (±3%) of framework Al vs total Al, as determined by ^{27}Al MAS NMR. [c] Relative integrated peak areas (±3%) of various hydroxyl groups, as determined by ^{1}H MAS NMR.

chemical shifts of ^{1}H, ^{13}C, and ^{29}Si were referenced to TMS, while that of ^{27}Al was referenced to 1 mol/L aqueous $Al(NO_3)_3$.

In addition, ^{1}H DQ MAS NMR spectra were carried out in a 5 mm MAS probe with a sample spinning rate of 10 kHz. DQ coherences were excited and reconverted with the POST-C7[50] pulse sequence following the general scheme of 2D MQ spectroscopy. The increment in the indirect dimension (t_1) was set to 20 μs, and 128 scans were acquired for each t_1 increment. The overall pulse phases for the excitation period were phase cycled according to the time-proportional phase-increment (TPPI)[51] procedure while the DQ MAS NMR spectra were recorded.

3. Results and Discussion

3.1. Effects of Calcination on Dealuminated H-Y Zeolites. Figure 1 displays the ^{1}H, ^{27}Al, and ^{29}Si MAS NMR spectra of H-Y zeolites before and after the calcination treatments. As compared to the parent H-Y zeolite, which reveals two main resonance peaks at 5.0 and 4.3 ppm and a weak shoulder peak at 2.2 ppm, up to five resonances at 5.0, 4.3, 2.8, 2.2, and 1.0 ppm were observed in the ^{1}H MAS spectra of calcined H-Y (Figure 1a). The peaks at 4.3 and 5.0 ppm can be assigned to the bridging SiOHAl groups (Brønsted acid sites) located in the supercages and sodalite cages of the calcined H-Y zeolite, respectively.[52] The signals at 2.8 and 1.0 ppm are due to the extraframework AlOH species (Lewis acid sites) in the supercages and sodalite cages, respectively, whereas the resonance at 2.2 ppm arises from the nonacidic silanols in the calcined H-Y zeolites.[53] The peak assignments and their corresponding integrated areas obtained from spectral deconvolution are depicted in Table 1. It is noted that, upon increasing the calcination temperature, notable decreases in the signal intensities of Brønsted acidic protons in both the sodalite cages (5.0 ppm) and the supercages (4.3 ppm) were observed. In addition, the peak area responsible for the extraframework AlOH species in the supercages (2.8 ppm) was found to increase with increasing calcination temperature, indicating a progressive release of Al atoms from the zeolite framework (forming more and more EFAL species). Interestingly, the signal intensity of the extraframework AlOH species in the sodalite cages (1.0 ppm) remains practically unchanged upon varying the calcination temperature, while that of the Brønsted acidic protons in the sodalite cages (5.0 ppm) gradually decreases, suggesting that some of the bridging hydroxyls (SiOHAl) in the sodalite cages were converted to EFAL species and migrate to the supercages upon progressive dealumination by calcination treatment.

As shown in Figure 1b, while the ^{27}Al MAS NMR spectrum of parent hydrated H-Y zeolite shows predominately resonance arising from tetrahedral (four-coordinated) framework Al species, additional resonance peaks at 30 and −2 ppm, which can be respectively attributed to five- and six-coordinated EFAL species, were evident for the calcined H-Y zeolite samples.[54,55] An additional ^{27}Al 2D multiple-quantum (MQ) MAS NMR[47] experiment performed on the dehydrated CAL-500 zeolite (see the Supporting Information, Figure S3) revealed the presence of four-coordinated framework Al, four-coordinated EFAL, five-coordinated EFAL, and six-coordinated EFAL.[54−56] That the integrated areas of the pentahedral (30 ppm) and octahedral (−2 ppm) EFAL peaks progressively increase with increasing

calcination temperature at the expense of the tetrahedral framework Al signal at 60 ppm clearly indicates the progressive increase in the extent of dealumination, in excellent agreement with the aforediscussed ^{1}H MAS NMR results. Likewise, results obtained from ^{29}Si MAS NMR provide additional support to the above findings. By deconvoluting the ^{29}Si NMR MAS spectra observed for the parent H-Y and CAL-400, CAL-500, CAL-600, and CAL-700 dealuminated samples (Figure 1c), their corresponding framework Si/Al ratios were determined to be 2.8, 3.0, 3.5, 4.6, and 5.3, respectively (Table 1), suggesting a progressive decrease in framework Al content with increasing calcination temperature. Thus, the results obtained from ^{1}H, ^{27}Al, and ^{29}Si MAS NMR experiments suggest that the higher the calcined temperature, the greater the extent of dealumination and hence the greater the amount of EFAL species present in the zeolite.

The two-dimensional ^{1}H DQ MAS NMR experiment has been known as a powerful technique for probing proton−proton proximities in various solid materials.[48,49] Since the DQ coherences observed are strongly dependent on the internuclear distance, the presence of a signal in the ^{1}H DQ MAS spectrum would indicate that the two protons should be in close proximity. Peaks that occur along the diagonal (ω, 2ω) axis therefore represent autocorrelation peaks arising from dipolar interactions of protons having the same chemical shift, whereas pairs of off-diagonal peaks at (ω_a, $\omega_a + \omega_b$) and (ω_b, $\omega_a + \omega_b$) would correspond to correlations between two protons with different chemical shifts. The ^{1}H DQ MAS NMR spectrum of parent H-Y zeolite (Figure 2a) reveals the existence of only two autocorrelation peaks at (4.3, 8.6) and (5.0, 10.0) ppm, which can be ascribed to spatial proximities between pairs of Brønsted acidic protons in the supercages and the sodalite cages of the dealuminated H-Y zeolite, respectively.[49] Upon dealumination treatment of the zeolite by calcination, additional autocorrelation peaks emerge in the spectra together with some off-diagonal peaks. The spectra observed for CAL-400 (Figure 2b) and CAL-500 (Figure 2c) samples are rather similar except for some variations in the intensity of various correlation peaks. In addition to the two autocorrelation peaks present in the spectrum of the parent H−Y zeolite, two additional autocorrelation peaks at (2.2, 4.4) and (2.8, 5.6) ppm were observed for these two dealuminated samples. The former peak at (2.2, 4.4) ppm indicates formation of silanol nests during the dealumination process, in which the silanol pairs are in close proximity, as illustrated in Scheme 1, whereas the latter peak at (2.8, 5.6) ppm can be attributed to the EFAL species such as AlOOH or $Al(OH)_2^+$ in close proximity or those containing more than one hydroxyl group such as $Al(OH)_3$ or $Al(OH)_2^+$. In addition, two pairs of off-diagonal peaks are also observed for CAL-400 and CAL-500 samples. The pair at (1.0, 6.0) and (5.0, 6.0) ppm corresponds to correlations between the adjacent pair of extraframework AlOH (Lewis acid sites) and bridging hydroxyl (Brønsted acid sites) groups in the sodalite cages, whereas the pair at (2.8, 7.1) and (4.3, 7.1) ppm reflects the correlations between the adjacent pair of Lewis and Brønsted acid sites in the supercages. Moreover, a weak off-diagonal peak at (4.3, 5.3) ppm is also observed, which corresponds to the spatial correlation between a Brønsted acid site in the supercages and a Lewis acid site in the sodalite cages. That no autocorrelation peak at (1.0, 2.0) ppm is present indicates that the corresponding EFAL species in the sodalite cages are most likely present in the form of isolated $AlOH^{2+}$ or AlOOH, rather than $Al(OH)_3$ or $Al(OH)_2^+$. Clearly, the 2D ^{1}H DQ MAS NMR experiment is capable of revealing detailed spatial correlations among

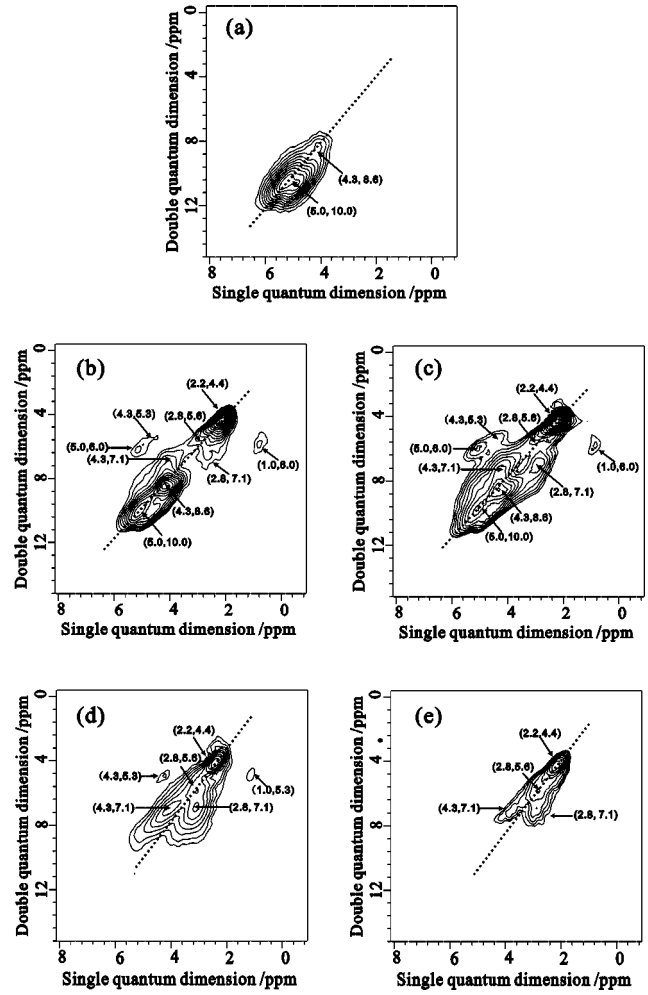

Figure 2. 2D ^{1}H DQ MAS NMR spectra of (a) parent H-Y, (b) CAL-400, (c) CAL-500, (d) CAL-600, and (e) CAL-700 zeolites.

SCHEME 1

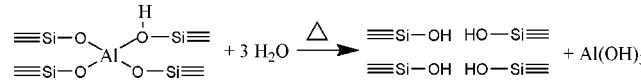

various hydroxyl groups in the calcined H-Y zeolites. The fact that correlations between the Lewis and Brønsted acid sites were observed also implies the existence of a synergy effect between the two types of acid sites in dealuminated zeolites.[49]

It is noted that the relative intensities of the autocorrelation peaks at (2.2, 4.4) and (2.8, 5.6) ppm increase while those of the peaks at (4.3, 8.6) and (5.0, 10.0) decrease upon increasing the calcination temperature from 400 to 500 °C. Such variations in the relative intensities of the autocorrelation peaks observed for dealuminated H-Y zeolites are consistent with the ^{1}H, ^{27}Al, and ^{29}Si MAS NMR results (vide supra), by which it can be inferred that more framework Al atoms were released from the structural framework with increasing severity of dealumination treatment. Consequently, this leads to an overall increase in the amount of EFAL species and silanol nets (see Scheme 1) in calcined H-Y and hence a decrease in the number of Brønsted acid pairs in close proximity. Meanwhile, the variations in the intensities of the cross-correlation peaks at (4.3, 7.1), (2.8, 7.1), (4.3, 5.3), (1.0, 6.0), and (5.0, 6.0) ppm with calcination temperature also provide additional support to the mechanism of Brønsted/Lewis acid synergy proposed earlier.[49]

Upon further increasing the calcination temperature above 500 °C, notable changes in the ^{1}H DQ MAS NMR spectra were

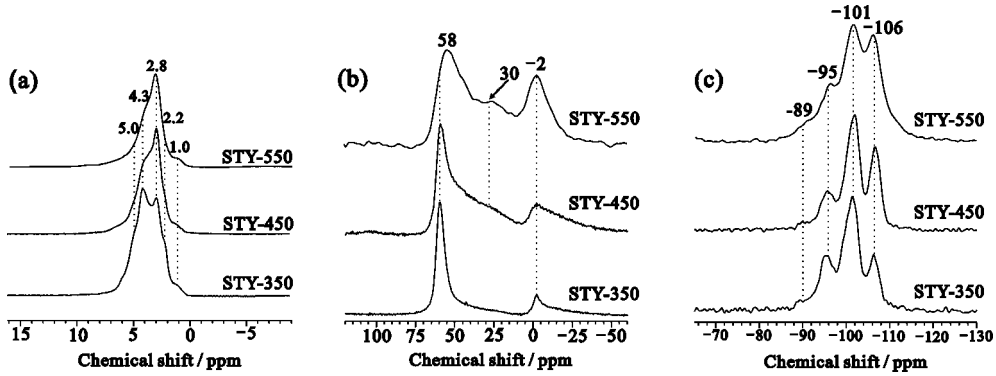

Figure 3. (a) ^{1}H, (b) ^{27}Al, and (c) ^{29}Si MAS NMR spectra of various dealuminated H-Y zeolites prepared with different steam treatment temperatures (350, 450, and 550 °C).

observed, as can be seen in parts d and e of Figure 2 for CAL-600 and CAL-700, respectively. First, it is obvious that the two autocorrelation peaks at (4.3, 8.6) and (5.0, 10.0) ppm are diminished in the 2D spectra, indicating that Brønsted acid sites in both the supercages and sodalite cages become isolated and no longer in close proximity when more and more Al atoms are released from the zeolite framework. Meanwhile, the pair of off-diagonal peaks at (5.0, 6.0) and (1.0, 6.0) ppm is also invisible, suggesting that Brønsted and Lewis acid sites are no longer in close proximity in the sodalite cage. Again, these observations are in line with the results shown in Figure 1 and Table 1, revealing that more Al atoms at Brønsted acid sites were being released in the sodalite cages than in the supercages. As such, Brønsted acid sites become less abundant and isolated, making their correlations with Lewis acid sites ineffective in the sodalite cages. In the case of CAL-600 (Figure 2d), spatial correlations between pairs of Brønsted and Lewis acid sites in the supercages [i.e., peak at (4.3, 7.1) ppm] and that between a Brønsted acid site in the supercage and a Lewis acid site in the sodalite cage [i.e., peak at (4.3, 5.3) ppm] still prevail in the calcined H-Y. However, upon further increasing the calcination temperature to 700 °C, apart from the two autocorrelation peaks at (2.2, 4.4) and (2.8, 5.6) ppm, only one pair of off-diagonal peaks at (4.3, 7.1) and (2.8, 7.1) ppm remains in the ^{1}H DQ MAS spectrum (Figure 2e), elucidating that the spatial correlations between the Brønsted and Lewis acid sites in the supercages prevail even at elevated calcination temperature.

To afford measurement of the average ^{1}H−^{1}H distance between various hydroxyl groups, additional ^{1}H DQ MAS NMR experiments were performed for the CAL-500 sample with varied DQ recoupling time (see the Supporting Information, Figure S4). Accordingly, the ^{1}H−^{1}H distance between a Brønsted acidic proton and a extraframework AlOH species in both the supercages and the sodalite cages was determined to be 4.3 Å, whereas that between a Brønsted acidic proton in the supercages and an extraframework AlOH species in the sodalite cages was measured to be 6.2 Å, which is slightly shorter compared to the value of 6.7 Å determined by theoretical DFT calculations[49] (see the Supporting Information, Table S1).

3.2. Effects of Steaming on Dealuminated H-Y Zeolites. The ^{1}H, ^{27}Al, and ^{29}Si MAS NMR spectra of dealuminated H-Y zeolites treated by steaming at different temperatures (350, 450, and 550 °C) shown in Figure 3 are in close resemblance to those of the calcined H-Y zeolites. As such, similar resonance assignments and arguments on the effect of the steaming temperature on variations of the NMR profiles (and hence the severity of dealumination) also prevail for steamed H-Y samples. However, by comparison to the calcined H-Y samples for which calcination temperatures within the range of 400−700 °C were

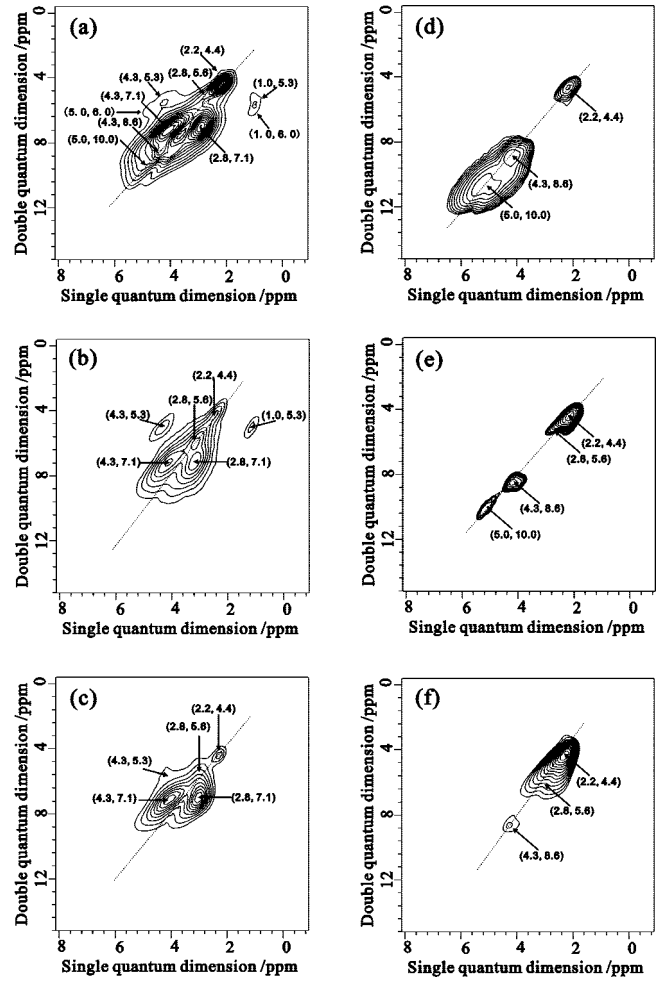

Figure 4. 2D ^{1}H DQ MAS NMR spectra of (a) STY-350, (b) STY-450, (c) STY-550, (d) OXA-0.2, (e) OXA-0.8, and (f) OXA-1.4 dealuminated H-Y zeolites.

examined, it appears that more severe dealuminations were made when the parent H-Y zeolite was treated in the presence of steam, even though the steamed samples were treated at relatively low temperatures (350−550 °C). This observation is also evidenced by the variations in the Si/Al ratios and relative intensities of various hydroxyl groups listed in Table 1. Parts a−c of Figure 4 show the 2D ^{1}H DQ MAS NMR spectra of steam-treated samples. Similar to the spectra observed for CAL-400 (Figure 2b) and CAL-500 (Figure 2c) samples, four diagonal peaks at (2.2, 4.4), (2.8, 5.6), (4.3, 8.6), and (5.0, 10.0) ppm were observed for the STY-350 sample together with three pairs of off-diagonal peaks at [(2.8, 7.1) and (4.3, 7.1)], [(1.0, 6.0),

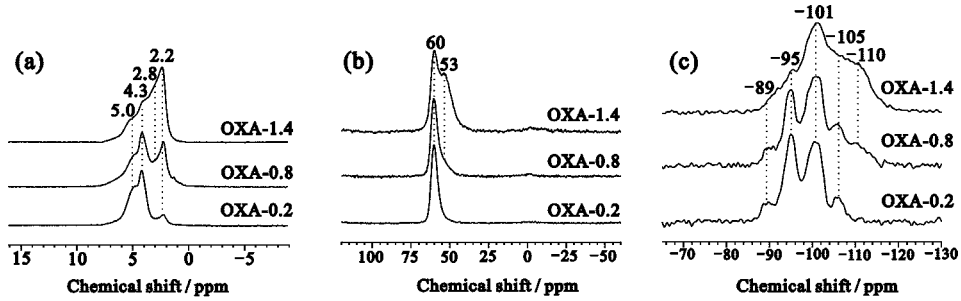

Figure 5. (a) ^{1}H, (b) ^{27}Al, and (c) ^{29}Si MAS NMR spectra of various dealuminated H-Y zeolites prepared by acid-leaching with oxalic acid under different acid concentrations (0.2, 0.8, and 1.4 mol/L).

(5.0, 6.0)], and [(1.0, 5.3), (4.3, 5.3)] ppm, as shown in Figure 4a. In this context, the first pair is associated with spatial correlations between a pair of Brønsted and Lewis acids in the supercages, the second pair is due to the spatial correlations between the Brønsted and Lewis acids in the sodalite cages, and the last pair corresponds to correlations between a Brønsted acid site in the supercages and a Lewis acid site in the sodalite cages.

By comparing the ^{1}H DQ MAS NMR spectra of samples with mild thermal treatments, for example, CAL-400 (Figure 2b) and STY-350 (Figure 4a), it is found that their correlation patterns are rather similar except for the slight variations in the intensities of various correlation peaks. Obviously, the correlation between the Brønsted and Lewis acid sites in the sodalite cages is relatively weaker in the STY-350 sample than the CAL-400 sample, probably due to the more severe extent of dealumination in the sodalite cages (see Table 1). It is noteworthy that the pair of off-diagonal peaks appearing at (1.0, 6.0) and (5.0, 6.0) ppm in the ^{1}H DQ MAS spectra of CAL-400 (Figure 2b) and CAL-500 (Figure 2c), which correspond to the Brønsted/Lewis correlations in the sodalite cages, is relatively weaker for steam-treated samples (Figure 4). Upon increasing the steaming temperature from 350 to 450 °C, the disappearance of the two autocorrelation peaks at (4.3, 8.6) and (5.0, 10) ppm in Figure 4b clearly reveals that dealumination treatment at elevated steaming temperatures results in isolation of Brønsted acids in both the supercages and the sodalite cages. Meanwhile, the two pairs of cross-correlation peaks appear to persist with increasing temperature of the hydrothermal dealumination treatment. As the steaming temperature is further raised to 550 °C (Figure 4c), correlations between the adjacent pair of Lewis and Brønsted acid sites in the supercages remain effective, while that between the Brønsted acid in the supercages and the Lewis acid in the sodalite cages becomes weaker.

3.3. Effects of Acid-Leaching on Dealuminated H-Y Zeolites. Although HCl and HNO_3 are commonly used for dealumination of zeolites,[57] oxalic acid was also found to be very effective in removing framework Al and EFAL species especially at relatively low concentrations.[10b,17,58,59] Figure 5 shows the ^{1}H, ^{27}Al, and ^{29}Si MAS NMR spectra of H-Y zeolite treated with oxalic acid under different acid concentrations (0.2, 0.8, and 1.4 mol/L). Unlike calcined (Figure 1a) and steam-treated (Figure 3a) dealuminated H-Y samples, the ^{1}H MAS NMR spectra of the acid-treated H-Y zeolites only show four resonance peaks at 5.0, 4.3, 2.8, and 2.2 ppm (Figure 5a). The resonance at 1.0 ppm is invisible, revealing the absence of EFAL species in the sodalite cages of acid-leached H-Y samples. The ^{27}Al spectrum observed for the OXA-0.2 sample prepared under modest acid treatment suggests the presence of only four-coordinated framework Al species, whereas in those for OXA-0.8 and OXA-1.4 samples an additional peak at ca. 53 ppm

SCHEME 2

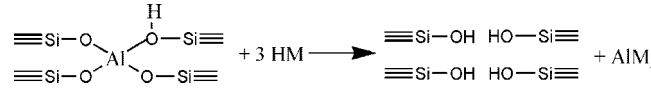

becomes visible, indicating the presence of four-coordinated EFAL.[17,58] By comparison to the ^{27}Al MAS NMR results obtained from the calcined (Figure 1b) and steam-treated (Figure 3b) H-Y zeolites, the absence of EFAL signals at 30 and −2 ppm observed for the acid-treated samples may be due to the fact that these EFAL species were effectively removed during the acid-leaching process, as illustrated in Scheme 2. Additional ^{1}H and ^{27}Al MAS NMR experiments performed on the acid-leached sample in the absence of water washing provide additional support to the above arguments (see the Supporting Information, Figure S5). As such, the extraframework AlOH species of the acid-treated samples should be present mostly in supercages rather than in the sodalite cages. As the concentration of oxalic acid increased, a notable gradual increase in the Si/Al ratio of the dealuminated zeolites was also observed (see Table 1). This may also be inferred from the ^{29}Si MAS NMR spectra of OXA-0.8 and OXA-1.4 samples in which a new resonance at −110 ppm due to the presence of an additional Q_4 site that is absent in the spectra of calcined (Figure 1c) and steam-treated (Figure 3c) H-Y zeolites was observed, in excellent agreement with previous reports.[17,60−62]

Parts d−f of Figure 4 display the ^{1}H DQ MAS NMR spectra of the acid-treated H-Y zeolites. Three diagonal peaks at (5.0, 10.0), (4.3, 8.6), and (2.2, 4.4) ppm can be observed for the OXA-0.2 sample (Figure 4d). Again, the former two autocorrelation peaks correspond to the spatial correlations between Brønsted acid sites in the supercages and the sodalite cages, respectively, while the latter peak is associated with the correlations between the silanol groups that are generated during the dealumination process. The absence of the autocorrelation peak at (2.8, 5.6) ppm (arising from the AlOH groups) in the 2D spectrum is likely due to the relatively low amount of EFAL species in the OXA-0.2 sample. It is noted that, at the expense of the signal intensities of the (4.3, 8.6) and (5.0, 10.0) ppm autocorrelation peaks, the peak at (2.8, 5.6) ppm emerges together with a notable increase in the intensity of the (2.2, 4.4) ppm peak upon increasing the concentration of oxalic acid to 0.8 mol/L during the dealumination treatment, as shown in Figure 4e. As the acid concentration was further increased to 1.4 mol/L, the peak at (5.0, 10.0) ppm accountable for correlations between Brønsted acid sites in the sodalite cages was diminished, while the peak at (4.3, 8.6) ppm further weakened. Unlike in calcined (Figure 2b−e) and steam-treated (Figure 4a−c) H-Y zeolites, none of the off-diagonal peaks arising from the spatial correlation between the acidic protons (Brønsted sites) and the EFAL hydroxyl groups (Lewis sites)

SCHEME 3

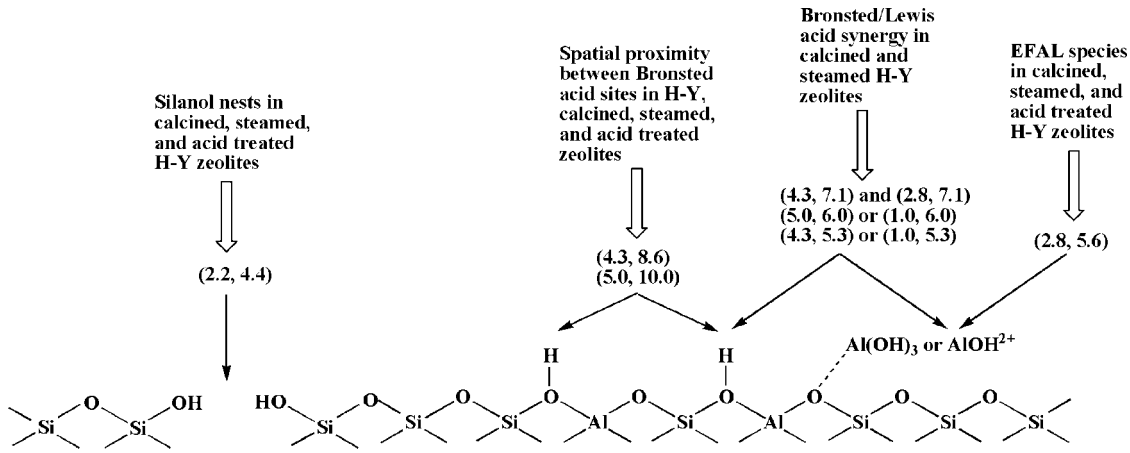

were observed, implying the absence of Brønsted/Lewis acid synergy in the acid-treated H-Y zeolites. A summary of the autocorrelation peaks observed for dealuminated H-Y zeolites modified by calcination, steaming, and acid-leaching treatments is illustrated in Scheme 3.

3.4. Variations in the Acid Strength for Various Dealuminated H-Y Zeolites. The Brønsted acid strengths of various dealuminated H-Y samples were further characterized by using $^{1}H \rightarrow {}^{13}C$ CP/MAS NMR of adsorbed 2-^{13}C-acetone.[33−35] The formation of a hydrogen bond between the Brønsted acidic proton and the carbonyl oxygen of adsorbed 2-^{13}C-acetone was found to result in a downfield shift of the carbonyl carbon. In other words, a higher ^{13}C chemical shift value observed by the adsorbed acetone would reflect a stronger acid strength of the Brønsted acid sites in zeolites. Figure 6 displays the ^{13}C CP/MAS NMR spectra of 2-^{13}C-acetone (0.2 mmol/g) adsorbed on the parent and various dealuminated H-Y zeolite samples. The spectrum observed for the parent H-Y zeolite (Figure 6a) shows only a single peak at 220 ppm, which can be ascribed due to acetone adsorbed on Brønsted acid sites. On the other hand, multiple resonance peaks were observed for calcined zeolites, as shown in Figure 6b−e. The broad resonance signals at 214, 183, 79, 74, and 30 ppm can be unambiguously attributed to the products formed through aldol reaction of acetone[33−35] (see the Supporting Information, Scheme S1), and the peaks appearing at 228 and 234 ppm have been previously assigned[49] to acetone adsorbed on Brønsted acid sites with stronger acid strengths (as compared to the peak at 220 ppm) that are interacting with Lewis acid sites, whereas the shoulder peak at ca. 241 ppm is likely associated with acetone directly adsorbed on Lewis acid sites. Similar results were also observed for steam-treated H-Y zeolites (Figure 6f−h). The presence of the two higher chemical shift peaks at 234 and 228 ppm in the ^{13}C spectra of calcined and steam-treated samples clearly indicates that the Brønsted acid strengths in these modified zeolite samples were greatly enhanced compared to that in their parent H-Y zeolite after the dealumination treatments. Such a phenomenon has been ascribed to the Brønsted/Lewis acid synergy effect, as also confirmed in our earlier study by theoretical DFT calculations.[49] As for the ^{13}C CP/MAS NMR spectra of 2-^{13}C-acetone loaded on acid-treated H-Y zeolites shown in Figure 6i,j, the peak at ca. 221 ppm can be assigned to acetone adsorbed on Brønsted acid sites and the signals at 30, 55, 73, 79, 178, 202, and 217 ppm to reaction products of acetone, whereas the

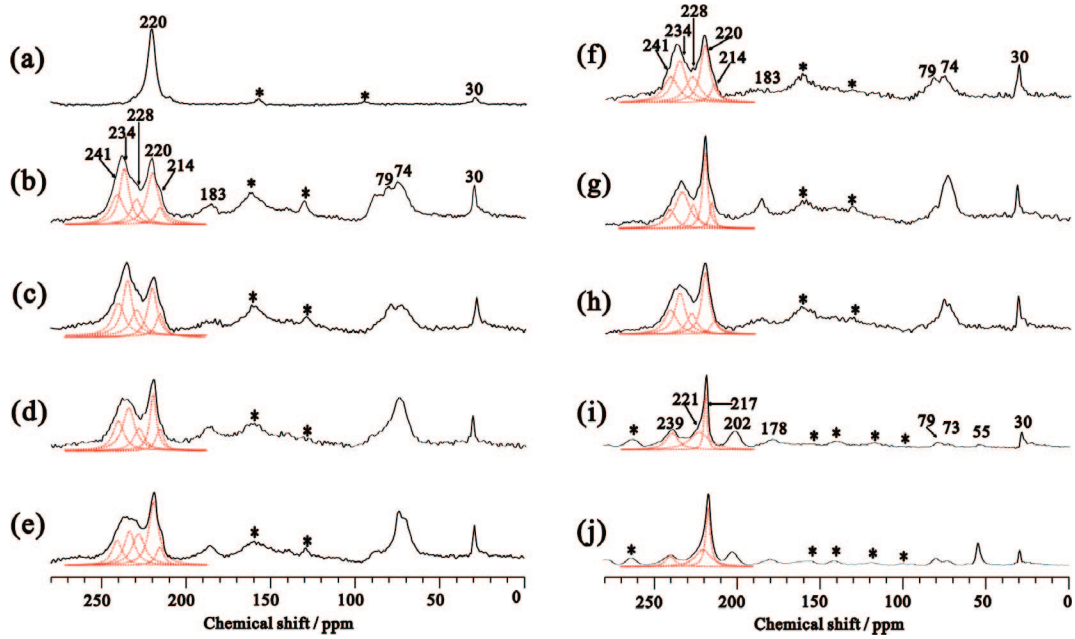

Figure 6. ^{13}C CP/MAS NMR spectra of 2-^{13}C-acetone adsorbed on (a) parent H-Y, (b) CAL-400, (c) CAL-500, (d) CAL-600, (e) CAL-700, (f) STY-350, (g) STY-450, (h) STY-550, (i) OXA−0.8, and (j) OXA-1.4 zeolites. Asterisks denote spinning sidebands.

downfield resonance at 239 ppm can be attributed to acetone directly adsorbed on Lewis acid sites. The fact that no ^{13}C resonance signals were observed in the chemical shift range of 228−234 ppm indicates that the Brønsted/Lewis acid synergy effect was absent in acid-treated H-Y zeolite samples, consistent with the above ^{1}H DQ MAS NMR results. Thus, the solid-state ^{13}C CP/MAS NMR experiment adopted herein using 2-^{13}C-acetone as the probe molecule not only facilitates discernment of Brønsted acid strengths in dealuminated H-Y zeolites but also is capable of identifying the occurrence of Brønsted/Lewis acid synergy.

4. Conclusions

We have demonstrated that the spatial proximities among various acid sites in H-Y zeolites modified by different dealumination treatments, viz., calcination, steam, and acid treatments, can be readily probed by 2D ^{1}H DQ MAS NMR in conjunction with conventional ^{1}H, ^{27}Al, and ^{29}Si MAS NMR and ^{13}C CP/MAS NMR spectra of adsorbed 2-^{13}C-acetone as the probe molecule. It is concluded that the properties of dealuminated H-Y zeolites vary with the method of dealumination used. In particular, the nature and location of EFAL species were rather different for samples modified by thermal, hydrothermal, and acid treatments. The EFAL species representing the Lewis centers were found to be more spatially connected with Brønsted acid sites in calcined and steam-treated zeolites compared to those dealuminated by acid-leaching. As such, dealuminated H-Y zeolites prepared by thermal and hydrothermal treatments tend to result in an enhancement of Brønsted acid strengths owing to the synergic effect between the Brønsted and the Lewis acid sites, whereas such an effect was not found in zeolites treated with oxalic acid. Furthermore, ^{13}C CP/MAS NMR of adsorbed 2-^{13}C-acetone is capable of not only probing the strengths of Brønsted acid sites in zeolites but also verifying the Brønsted/Lewis acid synergy. Though illustrated for H-Y zeolites in this study, the combined solid-state NMR techniques employed herein should also be applicable for probing the spatial proximities of acid sites in a variety of different solid acid catalysts.

Acknowledgment. This work was supported by the National Natural Science Foundation of China (Grants 20773159, 20673139, and 20425311) and by the National Science Council (NSC) (Grant NSC95-2113-M-001-040-MY3), Taiwan. S.-B.L. is grateful for a visiting professorship from the Wuhan Institute of Physics and Mathematics, Chinese Academy of Sciences, and A.Z. thanks the NSC and Institute of Atomic and Molecular Sciences, Academia Sinica, for a visiting research fellowship.

Supporting Information Available: Assorted ^{1}H, ^{27}Al, and ^{29}Si MAS NMR spectra of parent Na−Y and H−Y zeolites and dealuminated samples, 2D ^{27}Al MQ MAS NMR spectra of dehydrated CAL-500 zeolite, and details for estimation of $^{1}H-^{1}H$ distances for various hydroxyl groups in dealuminated zeolites. This material is available free of charge via the Internet at http://pubs.acs.org.

References and Notes

(1) Vaughan, D. E. W. In *Properties and Applications of Zeolites*; Townsend, R. P., Ed.; Society of Chemical Industry: London, 1980.

(2) Chen, N. Y.; Degnan, T. F.; Smith, C. M. *Molecular Transport and Reaction in Zeolites: Design and Application of Shape Selective Catalysts*; VCH Publishers: New York, 1994.

(3) Bhatia, S.; Beltramini, J.; Do, D. D. *Catal. Rev.—Sci. Eng.* **1989**−**1990**, *31*, 431.

(4) Davis, M. E. *Acc. Chem. Res.* **1993**, *26*, 111.

(5) Corma, A. *Chem. Rev.* **1995**, *95*, 559.

(6) (a) Zhao, Q.; Chen, W. H.; Huang, S. J.; Wu, Y. C.; Lee, H. K.; Liu, S. B. *J. Phys. Chem. B* **2002**, *106*, 4462. (b) Zhao, Q.; Chen, W. H.; Huang, S. J.; Liu, S. B. *Stud. Surf. Sci. Catal.* **2003**, *145*, 205.

(7) Bauer, F.; Chen, W. H.; Bilz, E.; Freyer, A.; Sauerland, V.; Liu, S. B. *J. Catal.* **2007**, *251*, 258.

(8) (a) Beyer, H. K. In *Molecular Sieves-Science and Technology*; Karge, H. G., Weitkamp, H., Eds.; Springer: Berlin, 2002; Vol. 3, p 203. (b) Triantafillidis, C. S.; Vlessidis, A. G.; Nalbandian, L.; Evmiridis, N. P. *Microporous Mesoporous Mater.* **2001**, *47*, 369.

(9) Parikh, P. A.; Subrahmanyam, N.; Bhat, Y. S.; Halgeri, A. B. *J. Mol. Catal.* **1994**, *88*, 85.

(10) (a) Maache, M.; Janin, A.; Lavalley, J. C.; Joly, J. F. *Zeolites* **1993**, *13*, 419. (b) Apellian, M. R.; Fung, A. S.; Kennedy, G. J.; Degnan, T. F. *J. Phys. Chem.* **1996**, *100*, 16577. (c) Xie, Z.; Chen, Q.; Zhang, C.; Bao, J.; Kao, Y. *J. Phys. Chem. B* **2000**, *104*, 2853.

(11) Beyer, H. K.; Belenykaja, I. *Stud. Surf. Sci. Catal.* **1980**, *5*, 203.

(12) Weitkamp, J.; Sakuth, M.; Chen, C.; Ernst, S. *J. Chem. Soc., Chem. Commun.* **1989**, 1908.

(13) (a) Skeels, G. W.; Breck, D. W. In *Proceedings of the 6th International Zeolite Conference*; Olson, D. H., Bisio, A., Eds.; Butterworths: Surrey, U.K., 1984; p 87. (b) Breck, D. W.; Blass, H.; Skells, G. W. U.S. Patent 4,503,203, 1985.

(14) (a) Kao, H. M.; Chen, Y. C. *J. Phys. Chem. B* **2003**, *107*, 3367. (b) Kao, H. M.; Chen, Y. C.; Ting, C. C.; Chen, P. T.; Jiang, J. C. *Catal. Today* **2004**, *97*, 13. (c) Kao, H. M.; Chang, P. C. *J. Phys. Chem. B* **2006**, *110*, 19104.

(15) (a) Kuhl, G. H. In *Molecular Sieves*; Uytterhoeven, J. B., Ed.; Lueven University Press: Leuven, Belgium, 1973; p 227. (b) Shannon, R. D.; Gardner, K. H.; Staley, R. H.; Bergeret, G.; Gallezot, P.; Auroux, A. *J. Phys. Chem.* **1985**, *89*, 4778.

(16) Datka, J.; Marschmeyer, S.; Neubauer, T.; Meusinger, J.; Papp, H.; Schütze, F. W.; Szpyt, I. *J. Phys. Chem.* **1996**, *100*, 14451.

(17) Yan, Z.; Ma, D.; Zhuang, J.; Liu, X.; Liu, X.; Han, X.; Bao, X.; Chang, F.; Xu, L.; Liu, Z. *J. Mol. Catal. A* **2003**, *194*, 153.

(18) Peixoto, D. P. B.; Cabral de Menezes, S. M.; Pais da Silva, M. I. *Mater. Lett.* **2003**, *57*, 3933.

(19) Triantafillidis, C. S.; Vlessidis, A. G.; Evmiridis, N. P. *Ind. Eng. Chem. Res.* **2000**, *39*, 307.

(20) Mota, C. J. A.; Martins, R. L.; Nogueira, L.; Kover, W. B. *J. Chem. Soc., Faraday Trans.* **1994**, *90*, 2297.

(21) Biaglow, A. I.; Parrillo, D. J.; Kokotailo, G. T.; Gorte, R. J. *J. Catal.* **1994**, *148*, 213.

(22) (a) Beyerlein, R. A.; ChoiFeng, C.; Hall, J. B.; Huggins, B. J.; Ray, G. J. *Top. Catal.* **1997**, *4*, 27. (b) Beyerlein, R. A.; McVicker, G. B.; Yacullo, L. N.; Ziemiak, J. J. *J. Phys. Chem.* **1988**, *92*, 1967.

(23) Corma, A.; Fornes, V.; Rey, F. *Appl. Catal.* **1990**, *59*, 267.

(24) Fritz, P. O.; Lunsford, J. H. *J. Catal.* **1989**, *118*, 85.

(25) Wang, Q. L.; Giannetto, G.; Guisnet, M. *J. Catal.* **1991**, *130*, 471.

(26) Viswanadham, N.; Gupta, J. K.; Dhar, G. M.; Garg, M. O. *Energy Fuels* **2006**, *20*, 1806.

(27) Yoo, K. S.; Gopal, S.; Smirniotis, P. G. *Ind. Eng. Chem. Res.* **2005**, *44*, 4562.

(28) Lopez, C. M.; Rodriguez, K.; Mendez, B.; Montes, A.; Machado, F. J. *Appl. Catal., A* **2000**, *197*, 131.

(29) Mirodatos, C.; Barthomeuf, D. *J. Chem. Soc., Chem. Commun.* **1981**, 39.

(30) Fabre, P. L.; Devynck, J.; Tremillon, B. *Chem. Rev.* **1982**, *82*, 591.

(31) (a) Klinowski, J. *Chem. Rev.* **1991**, *91*, 1459. (b) Fyfe, C. A.; Feng, Y.; Grondey, H.; Kokotailo, G. T.; Gies, H. *Chem. Rev.* **1991**, *91*, 1525. (c) Fyfe, C. A.; Mueller, K. T.; Kokotailo, G. T. In *NMR Techniques in Catalysis*; Bell, A. T., Pines, A., Eds.; Marcel Dekker: New York, 1994; p 11.

(32) (a) Pfeifer, H.; Freude, D.; Hunger, M. *Zeolites* **1985**, *5*, 274. (b) Hunger, M.; Freude, D.; Pfeifer, H. *J. Chem. Soc., Faraday Trans.* **1991**, *87*, 657. (c) Hunger, M. *Solid State Nucl. Magn. Reson.* **1996**, *6*, 1. (d) Hunger, M. *Catal. Rev.—Sci. Eng.* **1997**, *39*, 345.

(33) (a) Biaglow, A. I.; Gorte, R. J.; Kokotailo, G. T.; White, D. *J. Catal.* **1994**, *148*, 779. (b) Biaglow, A. I.; Šepa, J.; Gorte, R. J.; White, D. *J. Catal.* **1995**, *151*, 373. (c) Fărcaşiu, D.; Ghenciu, A. *Prog. Nucl. Magn. Reson. Spectrosc.* **1996**, *29*, 129.

(34) Zheng, A.; Chen, L.; Yang, J.; Zhang, M.; Su, Y.; Yue, Y.; Ye, C.; Deng, F. *J. Phys. Chem. B* **2005**, *109*, 24273.

(35) (a) Xu, T.; Munson, E. J.; Haw, J. F. *J. Am. Chem. Soc.* **1994**, *116*, 1962. (b) Xu, T.; Haw, J. F. *J. Am. Chem. Soc.* **1994**, *116*, 10188. (c) Haw, J. F.; Xu, T.; Nicholas, J. B.; Goguen, P. W. *Nature* **1997**, *389*, 832. (d) Xu, T.; Kob, N.; Drago, R. S.; Nicholas, J. B.; Haw, J. F. *J. Am. Chem. Soc.* **1997**, *119*, 12231.

(36) (a) Dawson, W. H.; Kaiser, S. W.; Ellis, P. D.; Inners, R. R. *J. Phys. Chem.* **1982**, *86*, 867. (b) Ripmeester, J. A. *J. Am. Chem. Soc.* **1983**, *105*, 2925. (c) Haw, J. W.; Chuang, I. S.; Hawkins, B. L.; Maciel, G. E. *J. Am. Chem. Soc.* **1983**, *105*, 7206. (d) Maciel, G. E.; Ellis, P. D. In *NMR*

Techniques in Catalysis; Bell, A. T., Pines, A., Eds.; Marcel Dekker: New York, 1994; p 231.

(37) (a) Baltusis, L.; Frye, J. S.; Maciel, G. E. *J. Am. Chem. Soc.* **1986**, *108*, 7119. (b) Baltusis, L.; Frye, J. S.; Maciel, G. E. *J. Am. Chem. Soc.* **1987**, *109*, 40.

(38) (a) Lunsford, J. H.; Rothwell, W. P.; Shen, W. *J. Am. Chem. Soc.* **1985**, *107*, 1540. (b) Lunsford, J. H. *Top. Catal.* **1997**, *4*, 91. (c) Zhao, B.; Pan, H.; Lunsford, J. H. *Langmuir* **1999**, *15*, 2761. (d) Hu, B.; Gay, I. D. *Langmuir* **1999**, *15*, 477. (e) Haw, J. F.; Zhang, J. H.; Shimizu, K.; Venkatraman, T. N.; Luigi, D. P.; Song, W. G.; Barich, D. H.; Nicholas, J. B. *J. Am. Chem. Soc.* **2000**, *122*, 12561.

(39) (a) Grey, C. P.; Veeman, W. S.; Vega, A. J. *J. Chem. Phys.* **1993**, *98*, 7711. (b) Kao, H. M.; Grey, C. P. *Chem. Phys. Lett.* **1996**, *259*, 459. (c) Kao, H. M.; Liu, H. M.; Jiang, J. C.; Lin, S. H.; Grey, C. P. *J. Phys. Chem. B* **2000**, *104*, 4923. (d) Kao, H. M.; Yu, C. Y.; Yeh, M. C. *Microporous Mesoporous Mater.* **2002**, *53*, 1. (e) Peng, L. M.; Chupas, P. J.; Grey, C. P. *J. Am. Chem. Soc.* **2004**, *126*, 12254. (f) Peng, L. M.; Grey, C. P. *Microporous Mesoporous Mater.*, in press.

(40) (a) Rakiewicz, E. F.; Peters, A. W.; Wormsbecher, R. F.; Sutovich, K. J.; Mueller, K. T. *J. Phys. Chem. B* **1998**, *102*, 2890. (b) Karra, M. D.; Sutovich, K. J.; Mueller, K. T. *J. Am. Chem. Soc.* **2002**, *124*, 902. (c) Osegovic, J. P.; Drago, R. S. *J. Catal.* **1999**, *182*, 1. (d) Osegovic, J. P.; Drago, R. S. *J. Phys. Chem. B* **2000**, *104*, 147.

(41) Chen, W. H.; Ko, H. H.; Sakthivel, A.; Huang, S. J.; Liu, S. H.; Lo, A. Y.; Tsai, T. C.; Liu, S. B. *Catal. Today* **2006**, *116*, 111.

(42) Luo, Q.; Deng, F.; Yuan, Z.; Yang, J.; Zhang, M.; Yue, Y.; Ye, C. *J. Phys. Chem. B* **2003**, *107*, 2435.

(43) Zheng, A.; Zhang, H. L.; Lu, X.; Liu, S. B.; Deng, F. *J. Phys. Chem. B* **2008**, *112*, 4496.

(44) Gullion, T.; Schaefer, J. *J. Magn. Reson.* **1989**, *81*, 196.

(45) Jarvie, T. P.; Wenslow, R. M.; Mueller, K. T. *J. Am. Chem. Soc.* **1995**, *117*, 570.

(46) Grey, C. P.; Vega, A. J. *J. Am. Chem. Soc.* **1995**, *117*, 8232.

(47) (a) Frydman, L.; Harwood, J. S. *J. Am. Chem. Soc.* **1995**, *117*, 5367. (b) Medek, A.; Harwood, J. S.; Frydman, L. *J. Am. Chem. Soc.* **1995**, *117*, 12779.

(48) (a) Brown, S. P. *Prog. Nucl. Magn. Reson. Spectrosc.* **2007**, *50*, 199. (b) Brown, S. P.; Spiess, H. W. *Chem. Rev.* **2001**, *101*, 4125.

(49) Li, S.; Zheng, A.; Su, Y.; Zhang, H.; Chen, L.; Yang, J.; Ye, C.; Deng, F. *J. Am. Chem. Soc.* **2007**, *129*, 11161.

(50) Hohwy, M.; Jakobsen, H. J.; Eden, M.; Levitt, M. H.; Nielsen, N. C. *J. Chem. Phys.* **1998**, *108*, 2686.

(51) (a) Drobnay, G.; Pines, A.; Dinton, S.; Weitekamp, D. P.; Wemmer, D. *Faraday Symp. Chem. Soc.* **1979**, *13*, 49. (b) Bodenhausen, G.; Vold, R. L.; Vold, R. R. *J. Magn. Reson.* **1980**, *37*, 93.

(52) Freude, D.; Hunger, M.; Pfeifer, H.; Schwieger, W. *Chem. Phys. Lett.* **1986**, *128*, 62.

(53) (a) Jiao, J.; Altwasser, S.; Wang, W.; Weitkamp, J.; Hunger, M. *J. Phys. Chem. B* **2004**, *108*, 14305. (b) Huang, J.; Jiang, Y.; Marthala, V. R. R.; Thomas, B.; Romanova, E.; Hunger, M. *J. Phys. Chem. C* **2008**, *112*, 3811.

(54) Van Bokhoven, J. A.; Koningsberger, D. C.; Kunkeler, P.; van Bekkum, H.; Kentgens, A. P. M. *J. Am. Chem. Soc.* **2000**, *122*, 12842.

(55) Jiao, J.; Kanellopoulos, J.; Wang, W.; Ray, S. S.; Foerster, H.; Freude, D.; Hunger, M. *Phys. Chem. Chem. Phys.* **2005**, *7*, 3221.

(56) Fyfe, C. A.; Bretherton, J. L.; Lam, L. Y. *J. Am. Chem. Soc.* **2001**, *123*, 5285.

(57) (a) Fernandes, L. D.; Monteiro, J. L. F.; Bartl, P. E.; Gusmão, J.; Menezes, S. C.; Cardoso, M. J. B. *Zeolites* **1994**, *14*, 533. (b) Trombetta, M.; Busca, G.; Storaro, L.; Lenarda, M.; Casagrande, M.; Zambon, A. *Phys. Chem. Chem. Phys.* **2000**, *2*, 3529. (c) Beers, A. E. W.; van Bokhoven, J. A.; de Lathouder, K. M.; Kapteijn, F.; Moulijn, J. A. *J. Catal.* **2003**, *218*, 239. (d) Gola, A.; Rebours, B.; Milazzo, E.; Lynch, J.; Benazzi, E.; Lacombe, S.; Delevoye, L.; Fernandez, C. *Microporous Mesoporous Mater.* **2000**, *40*, 73.

(58) Okada, K.; Arimitsu, N.; Karneshima, Y.; Nakajima, A.; MacKenzie, K. J. D. *Appl. Clay Sci.* **2006**, *31*, 185.

(59) (a) Müller, M.; Harvey, G.; Prins, R. *Microporous Mesoporous Mater.* **2000**, *34*, 135. (b) Giudici, R.; Kouwenhoven, H. W.; Prins, R. *Appl. Catal., A* **2000**, *203*, 101. (c) Bjørgen, M.; Bonino, F.; Kolboe, S.; Lillerud, K.-P.; Zecchina, A.; Bordiga, S. *J. Am. Chem. Soc.* **2003**, *125*, 15863. (d) Beers, A. E. W.; van Bokhoven, J. A.; de Lathouder, K. M.; Kapteijn, F.; Moulijn, J. A. *J. Catal.* **2003**, *218*, 239. (e) Xia, J.; Mao, D.; Tao, W.; Chen, Q.; Zhang, Y.; Tang, Y. *Microporous Mesoporous Mater.* **2006**, *91*, 33.

(60) Cherif, L.; El-Berrichi, F. Z.; Bengueddach, A.; Tougne, P.; Fraissard, J. *Colloids Surf., A* **2003**, *220*, 83.

(61) Siantar, D. P.; Millman, W. S.; Fripiat, J. J. *Zeolites* **1995**, *15*, 556.

(62) Brouwer, D. H.; Kristiansen, P. E.; Fyfe, C. A.; Levitt, M. H. *J. Am. Chem. Soc.* **2005**, *127*, 542.

JP803494N